

RESEARCH

Open Access



Impaired autophagy contributes to the aggravated deterioration of osteoarthritis articular cartilage by peroxisome proliferator-activated receptor α deficiency, associated with decreased ERK and Akt activation

Yang Zhou^{1,3†}, Li Li^{2†}, Xiaolei Chen¹, Qiubo Zhao¹, Ning Qu³, Bing Zhang³, Xin Jin^{3*} and Chun Xia^{1,3*}

Abstract

Background Although the chondroprotection of peroxisome proliferator-activated receptor α (PPAR α) activation against osteoarthritis (OA) has been revealed, the regulatory mechanism of PPAR α deficiency to aggravate osteoarthritic cartilage deterioration remains unclear. Here, we aimed to investigate whether and how autophagy is involved in OA pathological progression.

Methods Model of experimental OA was established using destabilization of the medial meniscus in PPAR α -KO 129S4/SvJae male mice, followed by histopathological detection of articular cartilage and immunohistochemistry detection of extracellular matrix (ECM) or autophagy-related signal molecules. Meanwhile, human OA chondrocytes obtained from total knee replacement surgery patients with OA were cultured with the pretreatment of IL-1 β , followed with the treatment of PPAR α agonist WY14643 and the detection of related signal molecules.

Results PPAR α deficiency aggravated cartilage damage with decreased LC3B level in combination with an increase in P62 level, accompanied with reduced p-Akt and p-ERK levels in PPAR α -KO mouse model of experimental OA. On the contrary, PPAR α activation by WY14643 promoted ECM synthesis in IL-1 β -treated human OA chondrocytes, accompanied with increased LC3B-II/I ratio and Beclin 1 level and decreased P62 and Bcl2 levels. Meanwhile, it was observed that activated ERK and Akt by PPAR α activation contributed to the enhancement of autophagy and ECM synthesis in human OA chondrocytes.

Conclusions Impaired autophagy contributed to the aggravated deterioration of osteoarthritis articular cartilage by PPAR α deficiency associated with the suppression of ERK and Akt, with an implication that triggering PPAR α activation ought to be a potential promising therapeutic target for OA therapy.

Keywords PPAR α deficiency, Autophagy, ERK and Akt activation, Mouse model of experimental OA, Human OA chondrocytes

[†]Yang Zhou and Li Li have contributed equally to this work.

*Correspondence:

Xin Jin

xinjin@xmu.edu.cn

Chun Xia

chunxia@xmu.edu.cn

Full list of author information is available at the end of the article



Introduction

Osteoarthritis (OA) is a persistent degenerative condition affecting the joints, leading to symptoms such as joint pain and potential difficulties with walking. Joint damage of OA may be partially attributed to extracellular matrix (ECM) degradation, which is secreted by chondrocyte. PPAR α , which is part of the class I nuclear receptors, is a member of the ligand-dependent transcription factor superfamily that modifies gene expression through its interaction with the retinoid X receptor [1] or in a DNA binding-independent manner [2] to regulate inflammatory responses [3–5], lipid and lipoprotein metabolism [6], oxidative stress [7] and apoptosis [8]. In recent years, studies have shown that PPAR α and autophagy have a regulatory role [9, 10]. It has implicated that PPAR α activation has a positive effect on the ECM synthesis of chondrocyte. In osteoarthritic cartilage, the activation of PPAR α reduces the inflammatory and destructive reactions [11]. Activation of the PPAR α pathway enhances the production of interleukin-1 (IL-1) receptor antagonist in chondrocytes treated with cytokines [12]. However, how PPAR α deficiency aggravates osteoarthritic cartilage deterioration remains unclear. Understanding the regulatory mechanism of PPAR α deficiency is benefit for OA therapy by PPAR α activation.

As a conserved cellular self-digestion process, autophagy could eliminate intracellular unnecessary proteins, pathogens, and damaged organelles to sustain cell survival. OA is one of the human diseases in which autophagy is especially significant in its pathogenesis [13–15]. It has been demonstrated that impaired autophagy could contribute to the pathogenesis of cartilage diseases. The impairment of autophagy caused by the repression of Mfn2 plays a significant role in the development of intervertebral disc degeneration in degenerated human nucleus pulposus tissues [16]. The severity of experimental OA is increased by REDD1 deficiency, which impairs autophagy and mitochondrial biogenesis in articular cartilage [17]. Hence, we hypothesize that the regulation of PPAR α deficiency on ECM might be linked to autophagy.

In this study, we observed the histopathological characteristics of articular cartilage and levels of signal molecules related to ECM and autophagy in a mouse model with experimentally induced OA called PPAR α -KO 129S4/SvJae. In addition, the regulatory mechanism of PPAR α activation by WY14643 linked to autophagy was investigated in IL-1 β -treated human OA chondrocytes. Our observations suggest that impaired autophagy contributed to the aggravated deterioration of osteoarthritic articular cartilage by PPAR α deficiency, associated with the activation of ERK and Akt, with an implication

that triggering PPAR α activation ought to be a potential promising therapeutic target for OA therapy.

Materials and methods

Antibodies and reagents

Abcam Inc (Cambridge, MA, USA) was the source of the antibodies for PPAR α , Collagen II, MMP13, ADAMTS5, and P62. Cell Signaling Technology Inc (Beverly, MA, USA) provided the antibodies for Akt, p-Akt (Ser473), ERK, p-ERK (Thr202/Tyr204), Beclin 1, and ERK inhibitor U0126. Sigma-Aldrich in China (Shanghai, China) supplied the antibody for Aggrecan, Akt inhibitor Triciribine (TCN), and autophagy inhibitor chloroquine diphosphate salt (CQ). Proteintech Group, Inc (Rosemont, IL, USA) provided the antibodies for LC3B and Bcl2. Recombinant human IL-1 β was obtained from PeproTech China (Suzhou, China) and β -actin was obtained from Shanghai Abways Biotechnology (Shanghai, China).

PPAR α -KO mouse model of experimental OA

A total of 32 male mice, including 8~10-week-old Wild Type (WT) mice and 8~10-week-old PPAR α knockout (PPAR α -KO) mice, weighing 26~30 g, were obtained from Jackson Laboratory #003580 (Bar Harbor, ME, USA). Before the experiment, all PPAR α -KO mice were identified using PCR (Additional file 2: Figure S1). The study was approved by the Committee on the Ethics of Animal Experiments of Xiamen University. Mice were given intraperitoneal injections of sodium pentobarbital (50 mg/kg) for anesthesia. The right hind knee of each mouse underwent destabilization of the medial meniscus (DMM) to induce the OA model (OA group), while the left knee underwent mocked surgery (Sham group), as previously described [18]. Mice were not euthanized by cervical dislocation until 4 week post-operation, at which point articular cartilage samples were collected for histopathological and immunohistochemical analyses.

Histopathological assay

The samples that were fixed in 4% paraformaldehyde for 48 h underwent decalcification in 10% EDTA-2Na for 3 weeks and were subsequently paraffin-embedded using the same method explained before [19]. Sagittal plane sections, with a thickness of three micrometers, were taken from the medial side of the joint and stained with Safranin O-Fast green stain. To measure the thickness of the articular cartilage, from the superficial zone to the subchondral bone, in the medial femur condyle and tibial plateau, Image-Pro Plus 6.0 software was utilized by two observers who were blind to the experiment. Subsequently, the OARSI histopathology assessment system was employed to evaluate the level of articular cartilage degeneration [20]. In the OARSI system, a grade of 0

indicates normal cartilage, while a higher grade (ranging from 1 to 24) indicates a greater level of biological cartilage degeneration.

Immunohistochemistry assay

As per the manufacturer's instruction (MAIXIN.BIO, Fuzhou, China), three-micrometer-thick sections were incubated overnight at 4 °C with primary antibodies: Aggrecan (1:600), Collagen (1:100), LC3B (1:100), P62 (1:100), p-Akt (1:50), and p-ERK (1:50) dilutions. After that, secondary antibodies were applied. The immunohistochemical reaction was visualized using diaminobenzidine and counterstained with haematoxylin. Photomicrographs were captured with OLYMPUS BX41 microscope equipped with a digital camera. The positive chondrocytes expressing LC3B, P62, p-Akt, and p-ERK were counted semi-automatically using Image-Pro Plus 6.0 Software, and the area was measured using Image J Software. Subsequently, the data were analyzed with Graph-Pad Prism version 5, as previously described [19].

Human OA chondrocyte isolation and culture

Once the Ethics Committee of Medical School, Xiamen University granted approval for this project and all patients involved provided informed consent, human OA cartilage was obtained from the anonymous waste material of 12 OA patients who were undergoing total knee replacement surgery (Additional file 1: Table S1). Prior to surgery, the OA patients had refrained from taking any non-steroidal anti-inflammatory drugs or steroids for a minimum of 2 weeks, and had not received any intra-articular injection for at least 1 month. The explants were then stored in liquid nitrogen for chondrocyte culture, as mentioned in previous literature [21, 22], primary chondrocytes were grown in DMEM (10% fetal bovine serum) until they reached 80% confluence, and then were used to seed 60-mm Petri dishes or 96-well plates. To maintain an inflammatory state in human OA chondrocytes, chondrocytes obtained from OA patients were consistently exposed to IL-1 β for the following experiments.

Western blotting analysis

As previously described, protein extracts were obtained by lysing and collecting cells through centrifugation [21, 23], the latter were subjected to SDS-PAGE (8–12%) and transferred to a PVDF membrane (GE Healthcare, Herfordshire, UK). The membrane was subjected to overnight incubation at 4 °C with different primary antibodies as needed, and was then treated with the appropriate secondary antibodies at room temperature for 1 to 2 h. The reactivity of the antibodies was detected using an enhanced chemiluminescence detection kit from Pierce, Rockford, IL, USA.

Transmission electron microscopy

The cells were collected and then centrifuged at 2000 \times g for 15 min at 4 °C. Afterwards, they were fixed for 2 h at 4 °C in 2.5% glutaraldehyde in 0.1 M PBS (PH7.4) following the same procedure as described before [21, 24]. The samples underwent dehydration and were then embedded in Embed-812 resin. To obtain 70 nm sections, an ultramicrotome (Leica EM UC7, LEICA, Shanghai, China) was used, and these sections were stained with uranyl acetate and lead citrate. The transmission electron microscope (Tecnai G2 Spirit BioTWIN, FEI Company, Hillsboro, Oregon, USA) was utilized to observe autophagic vacuoles.

Dimethylmethylene blue assay

Glycosaminoglycan (GAG) contents in culture medium were measured using dimethylmethylene blue assay. Cells were harvested by centrifugation to extract DNA. The culture medium was treated with 2 mg/ml papain in an HEPES buffered saline solution (HBS) for a duration of 12 h at a temperature of 60 °C. A standard of shark chondroitin sulfate from Sigma-Aldrich (St. Louis, MO, USA) was used, with a range of 0 to 70 ng. To each well of a 96-well plate, 20 μ l of a papain solution, as well as each standard and sample dilution in triplicate, were added sequentially. Following this, 200 μ l of a DMMB solution was added to each well and the plate was read at a wavelength of 630 nm using a spectrophotometer within a time frame of 10 min. The amount of GAGs was adjusted based on the DNA content, which was measured using an infinite M200 instrument (Tecan, Switzerland)[21, 25].

Statistical analysis

The mean \pm SD of at least three independent experiments in each cell experiment and 6 independent samples in each group of animal experiment were presented as the data. The statistical significance between the groups was assessed using the *t* test for comparisons between two groups and one-way analysis of variance (ANOVA) for comparisons among groups or more. Tukey's post hoc tests were conducted following the analysis, using GraphPad Prism version 5 (GraphPad Software, Inc, San Diego, CA, USA). A *p* value less than 0.05 was considered significant.

Results

PPAR α deficiency aggravated articular cartilage damage in PPAR α -KO mouse model of experimental OA

Safranin O-Fast green staining was used to identify the histological features of knee joints in PPAR α -KO mice following DMM. The image shown in Fig. 1A demonstrated the typical structure of the matrix and a proper distribution of

cells in the WT sample of the Sham group. Conversely, the PPAR α -KO sample from the Sham group showed a lack of continuity in the superficial zone of the articular cartilage and a depletion of matrix (indicated by reduced Safranin O staining) in the upper one-third of the cartilage. However, there was no difference in cartilage thickness (femoral condyle and medial tibial plateau) and OARSI Score (0–24) between WT and PPAR-KO samples of Sham group (Fig. 1B, C). Compared with WT sample of OA group, there were heavy loss of cartilage matrix and cells at superficial and middle layer in PPAR α -KO sample of OA group, concomitant with a significant difference of cartilage thickness and OARSI Score between WT and PPAR α -KO sample in OA group (Fig. 1B, C, $*p < 0.05$). In the meantime, we observed a noteworthy decrease in the thickness of cartilage and an increase in the OARSI score in the medial femoral condyle and medial tibial plateau of the OA group's WT sample when compared to the Sham group's WT sample. In the PPAR α -KO sample of the OA group, there was a significant decrease in cartilage thickness and an increase in OARSI score in the medial femoral condyle and medial tibial plateau compared to the PPAR α -KO sample of the Sham group (Fig. 1B, C, $*p < 0.05$). In addition, there was no difference in the area of Aggrecan and Collagen II expression between the WT and PPAR α -KO samples in the Sham group, but a significant difference was observed between the WT and PPAR α -KO sample of the OA group (indicated by the red arrows, Fig. 2A, B, $*p < 0.05$). Furthermore, the levels of Aggrecan and Collagen II in the WT sample of the OA group were lower than that in the WT sample of the Sham group. Comparing the PPAR α -KO sample of the Sham group, there was a significant decrease in Aggrecan and Collagen II levels in the PPAR α -KO sample of the OA group (Fig. 2A, B, $*p < 0.05$). Overall, the data indicate that PPAR α deficiency worsens articular cartilage damage, leading to reduced cellularity, Aggrecan, and Collagen II levels in the experimental OA mouse model, but not in the Sham group.

PPAR α deficiency decreased LC3B-II/I ratio in combination with an increase in the P62 level, with reduced p-ERK and p-Akt levels in PPAR α -KO mouse of experimental OA

In Sham group, compared with WT sample, chondrocytes in PPAR α -KO sample displayed a higher P62 level in combination with a lower LC3B level, but without significant difference (Fig. 3). In OA group, there was a significant increase in the P62 level with a decrease in LC3B level between PPAR α -KO and WT sample (indicated by the red

arrows, Fig. 3, $*p < 0.05$). In addition, in Sham group, the phosphorylation of ERK (p-ERK) and Akt (p-Akt) in chondrocytes of PPAR α -KO sample seemed to be lower than that of WT sample, but without significant difference (indicated by the red arrows, Fig. 4). In OA group, there were significant differences in p-ERK and p-Akt levels between PPAR α -KO and WT sample, expressing reduced p-ERK and p-Akt levels in PPAR α -KO sample (indicated by the red arrows, Fig. 4, $*p < 0.05$). Therefore, the data showed that PPAR α deficiency decreased LC3B level in combination with an increase in the P62 level, accompanied with reduced the levels of p-ERK and p-Akt in PPAR α -KO mice with OA.

PPAR α activation by WY14643 enhanced Aggrecan, and Collagen II levels accompanied with the alteration of LC3B-II/I ratio, Beclin1, P62, and Bcl2 levels in IL-1 β -treated human OA chondrocytes.

Figure 5A illustrates that Collagen II and Aggrecan levels increased, while MMP13 and ADAMTS5 levels decreased due to PPAR α activation by WY14643 ($*p < 0.05$, compared to the IL-1 β -treated group). In addition, activated PPAR α resulted in an increase in the LC3B-II/I ratio and a decrease in the P62 level, along with an increase in the Beclin1 level and a decrease in the Bcl2 level (Fig. 5A, $*p < 0.05$, compared to the IL-1 β -treated group). Furthermore, the addition of the autophagy inhibitor CQ partially attenuated the effect of WY14643, leading to a decrease in the Beclin 1 level and an increase in the P62 and Bcl2 levels, without significant changes in the LC3BII/I ratio (Fig. 5A, $*p < 0.05$, compared to the IL-1 β + WY14643-treated group). In Fig. 5B, it can be observed that GAG levels in the culture medium of IL-1 β + WY14643 human OA chondrocytes were higher than those in the IL-1 β -treated group; however, CQ diminished the effect of activated PPAR α by WY14643 on GAG as compared to the IL-1 β + WY14643-treated group ($*p < 0.05$). Using a transmission electronic microscope, it was observed that IL-1 β + WY14643-treated group had an increased number of autophagic vacuoles compared to the IL-1 β -treated group, whereas accumulation of autophagic vacuoles could be observed in the IL-1 β + WY14643 + CQ-treated group (Fig. 5C). In conclusion, these findings suggest that PPAR α activation by WY14643 enhances Aggrecan and Collagen II levels and alters the levels of Beclin 1, P62, and Bcl2 in IL-1 β -treated human OA chondrocytes.

(See figure on next page.)

Fig. 1 Aggravated cartilage damage in PPAR α -KO mouse model of experimental OA by DMM. **A** Sections in different treated groups were examined using Safranin O-Fast green stain (original magnification $\times 20$); **B** graph shows the change in articular cartilage thickness in medial femur condyle and tibial plateau. Data are mean \pm SD of eight joints per group ($*p < 0.05$); **C** graphs show the histopathological assay performed by OARSI histopathology assessment system in medial femur condyle and tibial plateau. Data are mean \pm SD of eight joints per group ($*p < 0.05$)

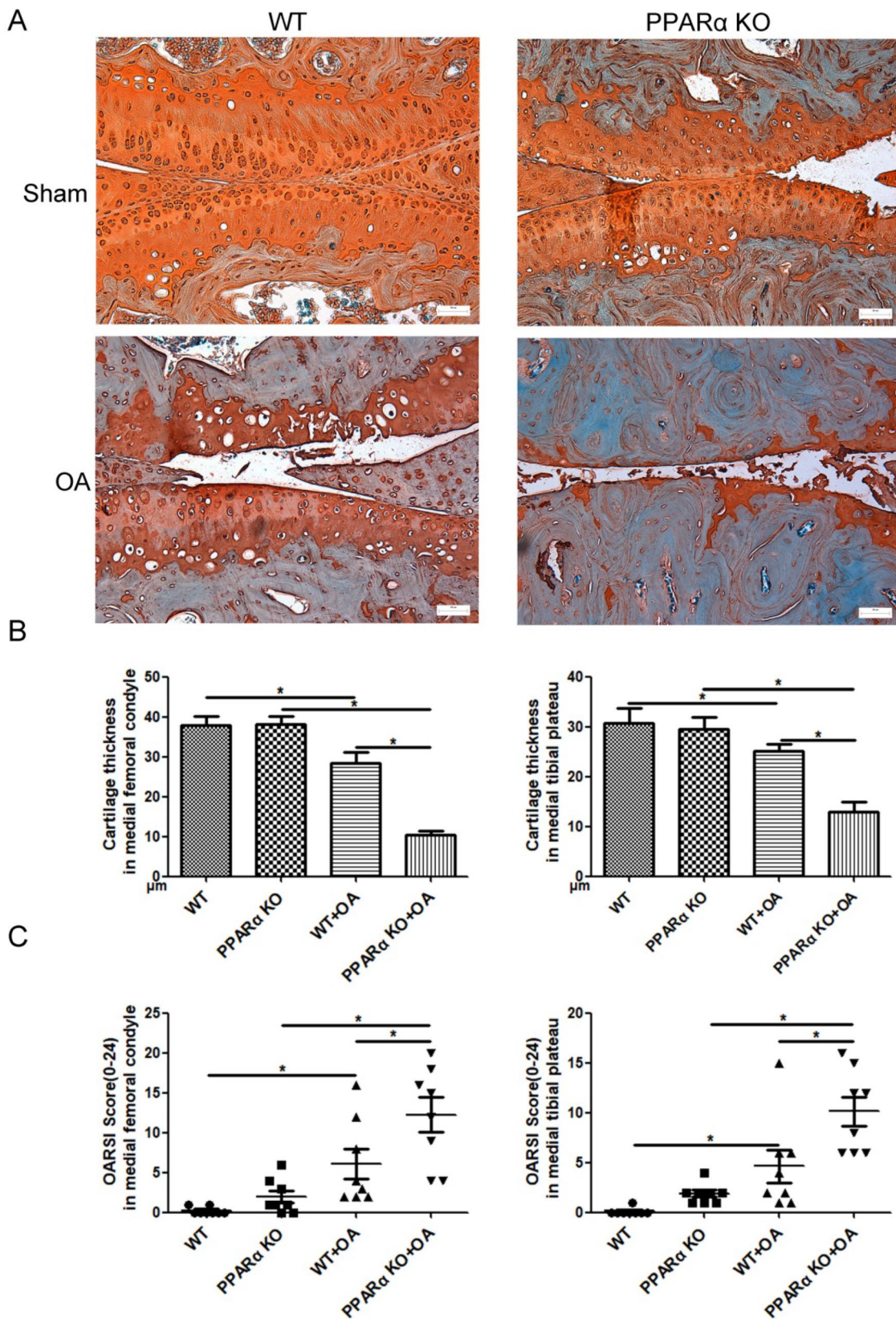


Fig. 1 (See legend on previous page.)

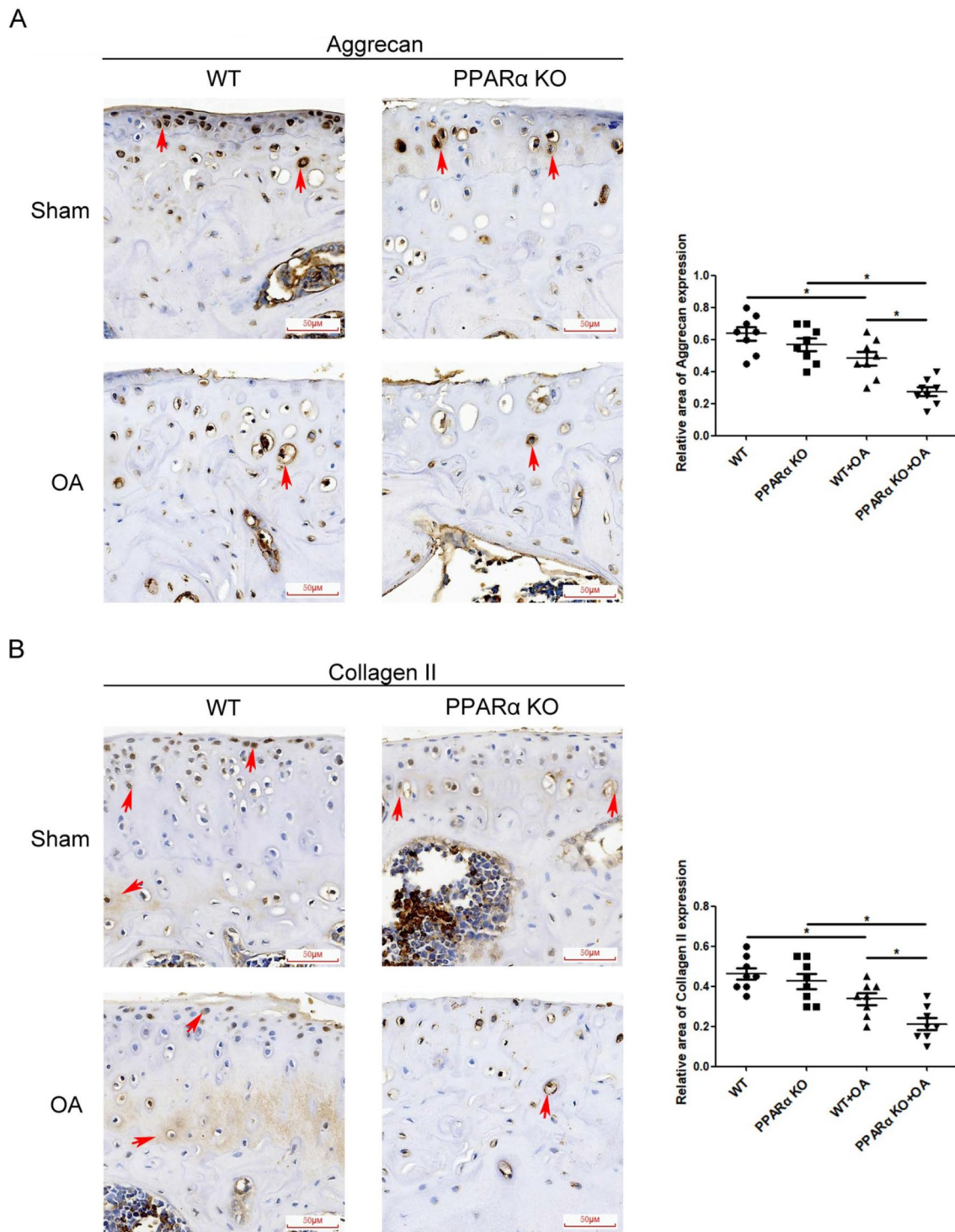


Fig. 2 Expression of ECM synthesis biomarkers in cartilage of PPAR α -KO mouse model of experimental OA. Sections in different treated groups were examined using immunohistochemistry assay; **A** representative image from mice of different treated groups expressing Aggrecan (original magnification $\times 40$). Graph shows the relative area expressing Aggrecan. Data are mean \pm SD of 24 fields of vision per group ($*p < 0.05$); **B** representative images from mice of different treated groups expressing Collagen II (original magnification $\times 40$). Graph shows the relative area expressing Collagen II. Data are mean \pm SD of 24 fields of vision per group ($*p < 0.05$)

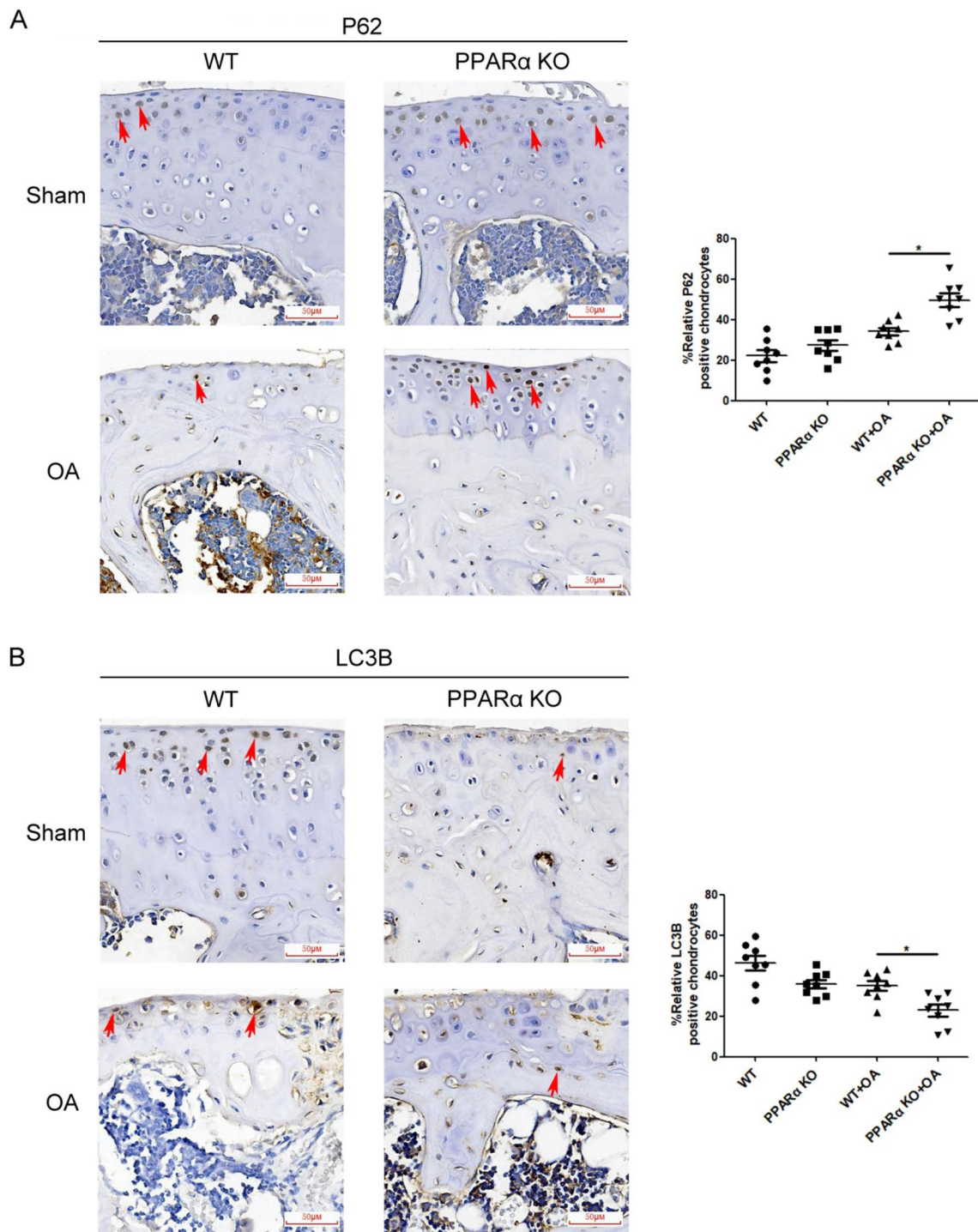


Fig. 3 Expression of autophagy biomarkers in cartilage of PPAR α -KO mouse model of experimental OA. Sections in different treated groups were examined using immunohistochemistry assay. **A** Representative image from mice of different treated groups expressing P62 (original magnification $\times 40$). Graph shows the percentage of positive chondrocytes expressing P62. Data are mean \pm SD of 500 cells per group ($*p < 0.05$); **B** representative images from mice of different treated groups expressing LC3B (original magnification $\times 40$). Graph shows the percentage of positive chondrocytes expressing P62. Data are mean \pm SD of 500 cells per group ($*p < 0.05$)

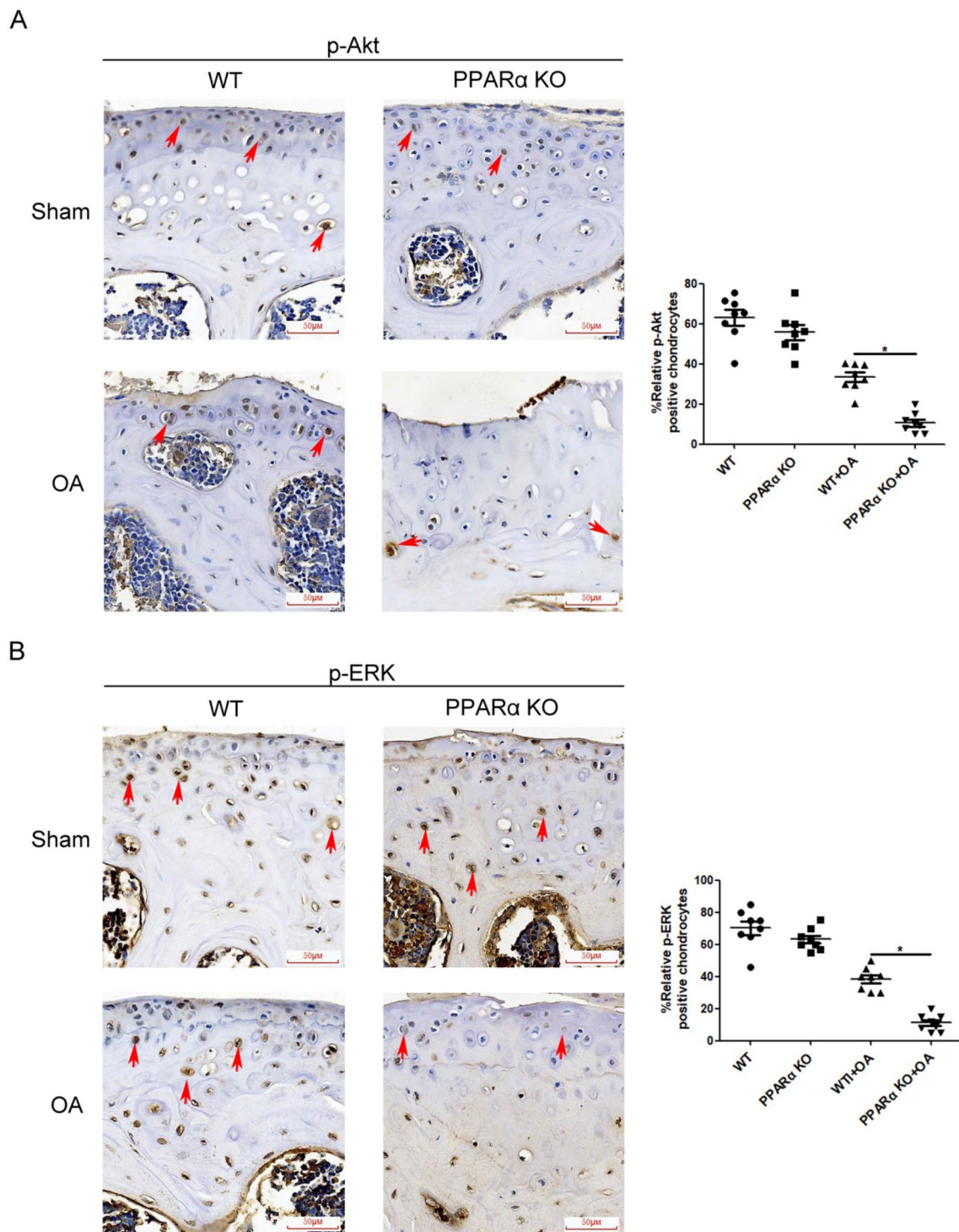


Fig. 4 Expression of p-ERK and p-Akt in cartilage of PPAR α -KO mouse model of experimental OA. Sections in different treated groups were examined using immunohistochemistry assay. **A** Representative image from mice of different treated groups expressing p-ERK (original magnification $\times 40$). Graph shows the percentage of positive chondrocytes expressing p-ERK. Data are mean \pm SD of 500 cells per group ($*p < 0.05$); **B** representative images from mice of different treated groups expressing LC3B (original magnification $\times 40$). Graph shows the percentage of positive chondrocytes expressing P62. Data are mean \pm SD of 500 cells per group ($*p < 0.05$)

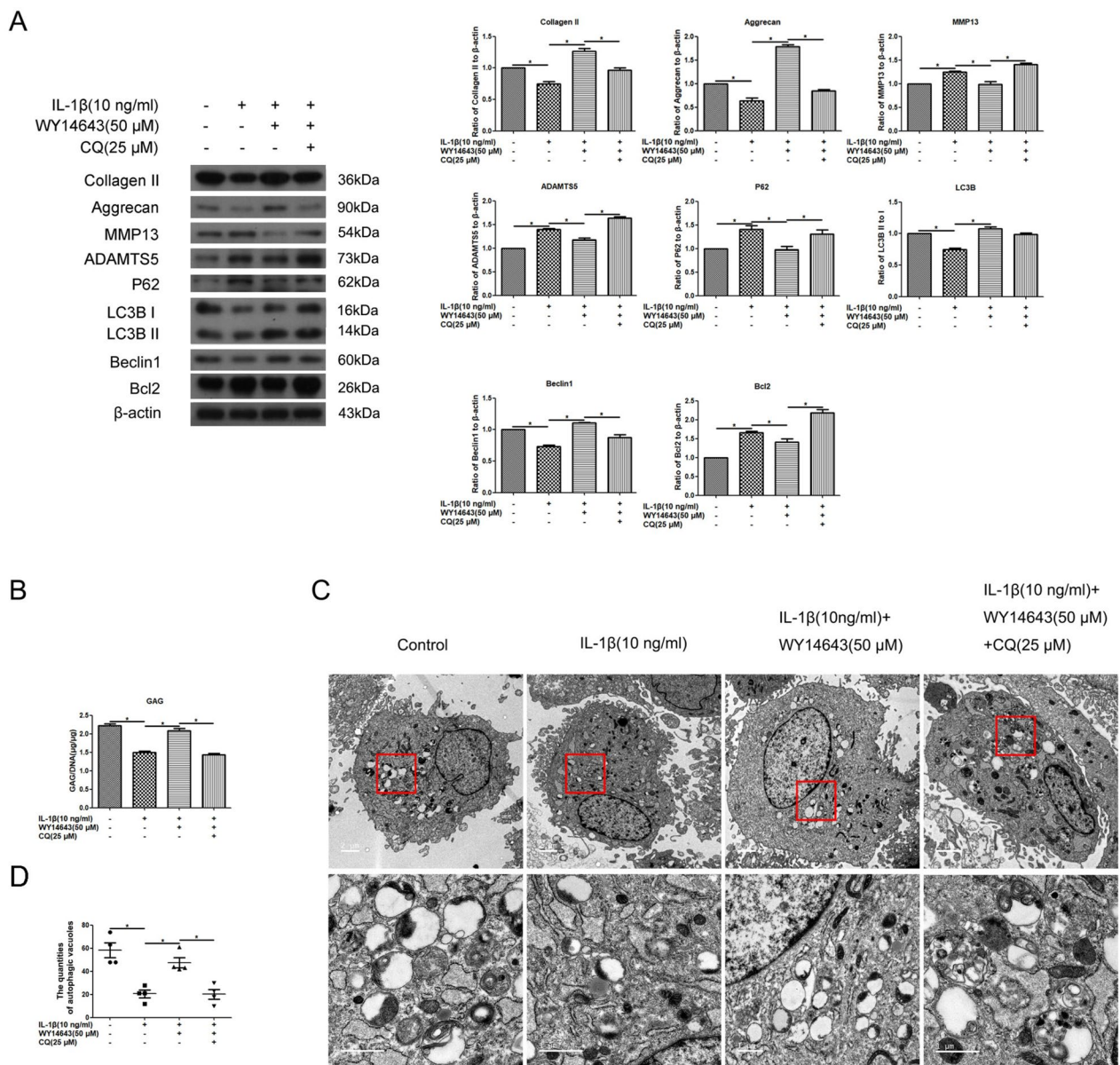


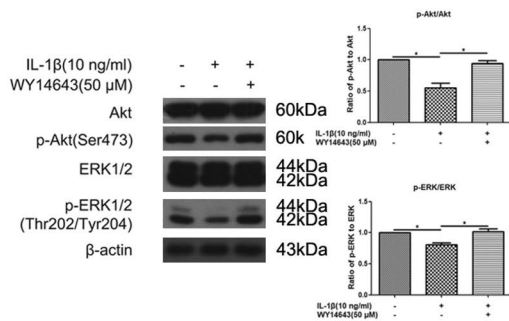
Fig. 5 Effect of PPAR α activation by WY14643 on the expression of ECM and autophagy-related signal molecules in IL-1 β -treated human OA chondrocytes. Cells were pretreated with WY14643 (50 μ M), CQ (10 μ M) or WY14643 (50 μ M) + CQ (10 μ M) for 2 h, respectively, and were then co-treated with IL-1 β (10 ng/ml) for 22 h. **A** Expression of Collagen II, Aggrecan, MMP13, ADAMTS5, P62, LC3B, Beclin1, Bcl2, and β -actin protein levels were detected via western blotting; **B** GAG levels were measured via Dimethylmethylene blue assay; **C** autophagic vacuoles were observed under a transmission electron microscope; **D** quantities of autophagic vacuoles. The data are representative of three independent experiments (* $p < 0.05$)

PPAR α activation by WY14643 elevated the phosphorylation of ERK and Akt in IL-1 β -treated human OA chondrocytes

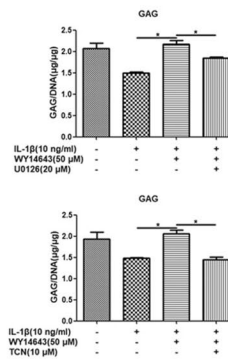
Activated PPAR α by WY14643 in IL-1 β -treated human OA chondrocytes increased the phosphorylation of ERK and Akt, as well as GAGs levels (Fig. 6A, * $p < 0.05$, vs IL-1 β -treated group). The addition of ERK inhibitor U0126 or Akt inhibitor TCN partially reduced the

upregulated p-ERK and p-Akt, as well as increased GAGs levels by activated PPAR α (Fig. 6B–D, * $p < 0.05$, vs IL-1 β + WY14643-treated group). Moreover, both U0126 and TCN reversed the effect of activated PPAR α on ECM and autophagy-related biomarkers (Collagen II, Aggrecan, MMP13, ADAMTS5, LC3B, P62, Beclin1, Bcl2) (Fig. 6C, and D, * $p < 0.05$). Consequently, PPAR α activation by WY14643 increased

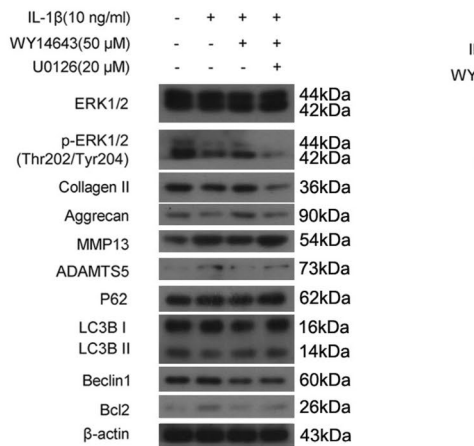
A



B



C



D

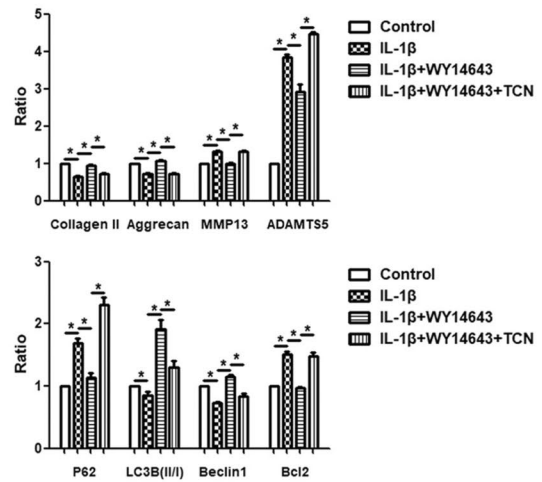
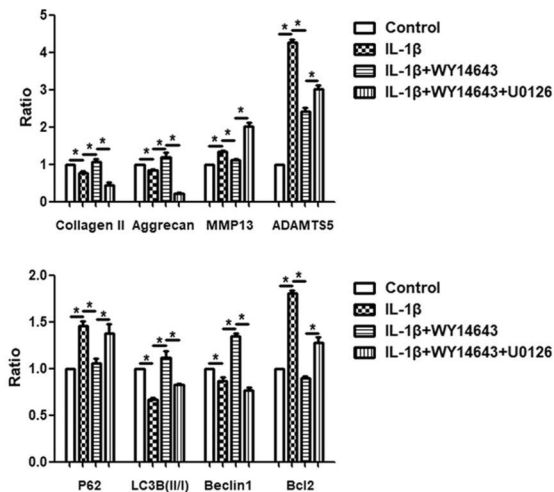
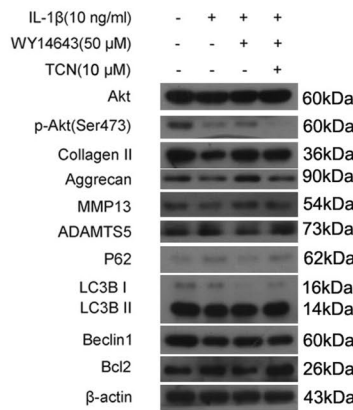


Fig. 6 Expression of p-ERK and p-Akt in IL-1 β -treated human OA chondrocytes. **A** Cells pretreated with WY14643 (50 μ M) for 2 h were co-treated with IL-1 β (10 ng/ml) for 22 h. The expression of Akt, p-Akt, ERK, p-ERK, and β -actin protein levels were detected via western blotting; **B** cells were pretreated with WY14643 (50 μ M), U0126 (20 μ M), WY14643 (50 μ M) + U0126 (20 μ M) and WY14643 (50 μ M) + TCN (10 μ M) for 2 h, respectively, and were then co-treated with IL-1 β (10 ng/ml) for 22 h. GAG levels were measured via Dimethylmethylene blue assay; **C** cells were pretreated with WY14643 (50 μ M), U0126 (20 μ M) or WY14643 (50 μ M) + U0126 (20 μ M) for 2 h, respectively, and were then co-treated with IL-1 β (10 ng/ml) for 22 h. The expression of ERK, p-ERK, Collagen II, Aggrecan, MMP13, ADAMTS5, P62, LC3B, Beclin1, Bcl2, and β -actin protein levels were detected via western blotting; **D** cells were pretreated with WY14643 (50 μ M), TCN (20 μ M) or WY14643 (50 μ M) + TCN (10 μ M) for 2 h, respectively, and were then co-treated with IL-1 β (10 ng/ml) for 22 h. The expression of Akt, p-Akt, Collagen II, Aggrecan, MMP13, ADAMTS5, P62, LC3B, Beclin1, Bcl2, and β -actin protein levels were detected via western blotting. The data are representative of three independent experiments (* p < 0.05)

the phosphorylation of ERK and Akt in IL-1 β -treated human OA chondrocytes.

Discussion

The primary finding of this study is that the absence of PPAR α in mice increased the severity of experimental OA. In comparison with the control group, the PPAR α -KO mouse model experienced more significant deterioration of the articular cartilage, resulting in reduced cellularity, Aggrecan, and Collagen II levels. Conversely, the use of WY14643, a PPAR α activator, was found to increase the levels of Aggrecan and Collagen II in human OA chondrocytes treated with IL-1 β . Taking into consideration the advantages and disadvantages of these results, it emphasizes the crucial role of PPAR α in the progression of OA.

It has been suggested that PPAR α activation provides defense against inflammatory reactions. For instance, the activation of PPARs, namely, α , β/δ , and γ , inhibits collagen production induced by TGF- β 1 and adjusts the balance between TIMP-1 and MMPs in chondrocytes cultured in three dimensions [26]. In chondrocytes, the expression of TGF- β and MMP-9 is reduced by PPAR α in response to AGE stimulation [27]. The activation of PPAR α pathway enhances the production of interleukin-1 β receptor antagonist in cytokine-treated chondrocytes [12]. The main function of PPAR is to directly or indirectly promote the inactivation of NF- κ B during inflammatory reactions [28]. In agreement with these studies, our findings in human OA chondrocytes also demonstrated that PPAR α activation by WY14643 enhanced Aggrecan, and Collagen II levels. Because of the protection by PPAR α activation, there were some signs of cartilage damage in articular cartilage in Sham PPAR α KO mice without DMM operation, such as the loss of ECM and aberrant cellular architecture.

Mounting evidence supports that autophagy is an important regulator of OA pathogenesis [14, 29, 30]. Another finding of this study is that PPAR α deficiency impaired autophagy in chondrocyte of experimental OA in mice. Compared to WT mice, the PPAR α -KO mouse model of experimental OA induced by DMM showed a decrease in autophagy, which was observed through a reduction in LC3B level and an increase in P62 level. Furthermore, our previous research has demonstrated that when WY14643 activates PPAR α , it results in an elevated LC3B-II/I ratio and a reduction in P62 levels in mouse chondrocytes treated with LPS and in an OA model [19], and we demonstrate that in IL-1 β -treated human OA chondrocytes, the activation of PPAR α resulted in an elevation of the Beclin1 level and a reduction in the Bcl2 level. This suggests that PPAR α activation also enhances autophagy by disrupting the Beclin1–Bcl2 complex.

It is widely recognized that Bcl-2/Bcl-XL can hinder autophagy by competing with Beclin-1 [23, 31]. This discovery provided more insight into the mechanisms that controlled autophagy in chondrocytes and emphasized the significance of PPAR α in regulating autophagy through various pathways.

PPAR α activation by its ligands could activate ERK in a variety of different cell types [32, 33]. Meanwhile, activating ERK by extracellular factors, such as cisplatin [34] and Platycodin D [35] could promote autophagy in cancer cells. Thus, it is believed that ERK activation associated with PPAR α might positively regulate autophagy. Here, PPAR α –ERK pathway partially contributed to autophagy enhancement in human OA chondrocyte. However, in contrast to the observation made by Ravingerová et al. in WY14643-treated rats' ischaemic myocardium, we noticed an increase in Akt phosphorylation in human OA chondrocytes treated with WY14643 [36]. Combining our findings that the Akt inhibitor TCN reversed the impact of activated PPAR α by WY14643 on biomarkers related to ECM and autophagy, it indicates that the PPAR α –Akt pathway may enhance autophagy to stimulate ECM synthesis in human OA chondrocytes. Despite Akt typically being known for its negative role in regulating autophagy, some studies have suggested the opposite. Lu et al. reported that rasfonin boosts autophagy by simultaneously reducing mTORC1 signaling and increasing Akt activity through the glycolytic pathway [37]; Dou et al. testify that the class IA phosphatidylinositol 3-kinase p110- β subunit acts upstream of Akt to trigger autophagy [38]. Akt might execute different or opposite functions in autophagy regulation, presumably due to different cell contexts and metabolic states.

A limitation to this study is the lack of precisely targeting PPAR α activation in articular chondrocyte in mouse model of experimental OA. Another one is that we did not investigate the effect of PPAR α agonist combined with autophagy activator on cartilage ECM synthesis in animal model of experimental OA. Last one is that we did not provide new insights into the molecular mechanism, except for the relationship between PPAR α and autophagy.

Conclusions

The deterioration of cartilage with impaired autophagy was further exacerbated by the absence of PPAR α , as confirmed by our findings. The activation of PPAR α with WY14643 stimulated autophagy by engaging ERK and Akt, leading to an increase in LC3B-II/I ratio, a decrease in P62 level, and the separation of Beclin1 from the Beclin1–Bcl2 complex. This ultimately enhanced the synthesis of ECM in chondrocytes affected by OA (Fig. 7). Consequently, initiating the activation of PPAR α should

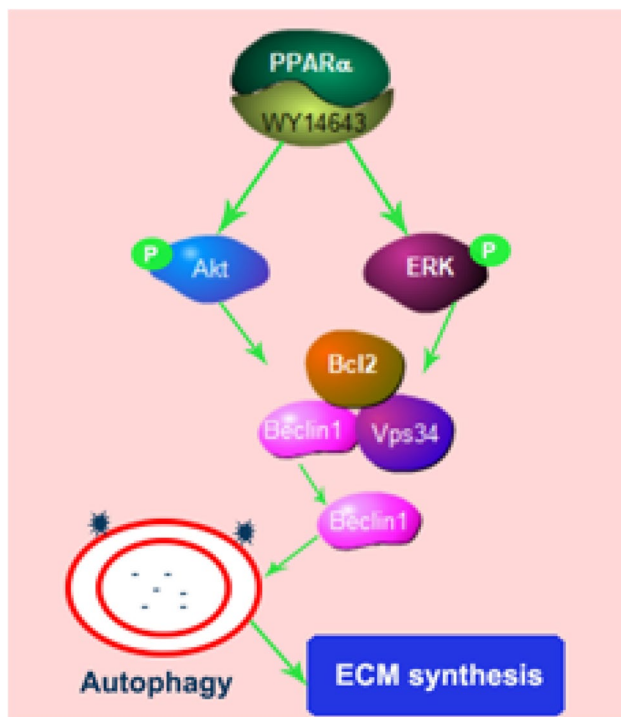


Fig. 7 Schematic depiction of proposed mechanism by which PPAR α -driven autophagy confers protection against OA in human OA chondrocytes and PPAR α -KO mouse model of experimental OA

be considered as a potentially effective target for treating OA.

Supplementary Information

The online version contains supplementary material available at <https://doi.org/10.1186/s40001-023-01267-4>.

Additional file 1: Table S1. Patient information for individuals undergoing total knee replacement surgery.

Additional file 2: Figure S1. PCR for PPAR α -KO mice Gene identification.

Acknowledgements

Not applicable.

Author contributions

YZ and LL performed most experiments and analyzed the data. BZ and CX designed and conducted the research and wrote the manuscript. XC and QZ carried out rest of animal experiments and data analysis. XJ and NQ participated in its design and coordination. All authors read and approved the final manuscript.

Funding

This study was supported by the National Science Foundation of China (No. 81972091) and Fujian Natural Science Foundation Youth Program (No. 2022J05293).

Availability of data and materials

The data sets used and/or analyzed during the current study are available from the corresponding author upon reasonable request.

Declarations

Ethics approval and consent to participate

Xiamen University's committee on the Ethics of Animal Experiments (XMU-LAC20180039) and the Ethics Committee of School of Medicine, Xiamen University (XMUMRE20170312), China, have approved the study. All procedures conducted in this study adhered to the 1964 Declaration of Helsinki and its subsequent revisions. We obtained written informed consent from all participants enrolled in the study.

Competing interests

The authors declare no competing interests.

Author details

¹Bone & Joint Research Institute, Zhongshan Hospital, Xiamen University, Xiamen 361102, China. ²Department of Orthopedics, Traditional Chinese Medical Hospital of Xinjiang Uygur Autonomous Region, Urumqi 830000, China.

³School of Medicine, Xiamen University, Xiamen 361102, China.

Received: 9 February 2023 Accepted: 4 August 2023

Published online: 09 September 2023

References

- DiRenzo J, Söderstrom M, Kurokawa R, Ogliastrro MH, Ricote M, Ingrey S, et al. Peroxisome proliferator-activated receptors and retinoic acid receptors differentially control the interactions of retinoid X receptor heterodimers with ligands, coactivators, and corepressors. *Mol Cell Biol*. 1997;17:2166–76.
- Rakhshandehroo M, Knoch B, Müller M, Kersten S. Peroxisome proliferator-activated receptor alpha target genes. *PPAR Res*. 2010;2010: 612089.
- Delerive P, De Bosscher K, Besnard S, Vanden Berghe W, Peters JM, Gonzalez FJ, et al. Peroxisome proliferator-activated receptor alpha negatively regulates the vascular inflammatory gene response by negative cross-talk with transcription factors NF-kappaB and AP-1. *J Biol Chem*. 1999;274:32048–54.
- Devchand PR, Keller H, Peters JM, Vazquez M, Gonzalez FJ, Wahli W. The PPARalpha-leukotriene B4 pathway to inflammation control. *Nature*. 1996;384:39–43.
- Staels B, Koenig W, Habib A, Merval R, Lebret M, Torra IP, et al. Activation of human aortic smooth-muscle cells is inhibited by PPARalpha but not by PPARgamma activators. *Nature*. 1998;393:790–3.
- Staels B, Dallongeville J, Auwerx J, Schoonjans K, Leitersdorf E, Fruchart JC. Mechanism of action of fibrates on lipid and lipoprotein metabolism. *Circulation*. 1998;98:2088–93.
- Yaribeygi H, Mohammadi MT, Jamialahmadi T, Sahebkar A. PPAR- α agonist fenofibrate ameliorates oxidative stress in testicular tissue of diabetic rats. *Crit Rev Eukaryot Gene Expr*. 2020;30:93–100.
- Chinetti G, Griglio S, Antonucci M, Torra IP, Delerive P, Majd Z, et al. Activation of proliferator-activated receptors alpha and gamma induces apoptosis of human monocyte-derived macrophages. *J Biol Chem*. 1998;273:25573–80.
- Kumari R, Ray AG, Mukherjee D, Chander V, Kar D, Kumar US, et al. Downregulation of PTEN promotes autophagy via concurrent reduction in apoptosis in cardiac hypertrophy in PPAR α (-/-) mice. *Front Cardiovasc Med*. 2022;9: 798639.
- Luo R, Su LY, Li G, Yang J, Liu Q, Yang LX, et al. Activation of PPAR α -mediated autophagy reduces Alzheimer disease-like pathology and cognitive decline in a murine model. *Autophagy*. 2020;16:52–69.
- Clockaerts S, Bastiaansen-Jenniskens YM, Feijt C, Verhaar JA, Somville J, De Clerck LS, et al. Peroxisome proliferator activated receptor alpha activation decreases inflammatory and destructive responses in osteoarthritic cartilage. *Osteoarthr Cartil*. 2011;19:895–902.
- François M, Richette P, Tsagris L, Fitting C, Lemay C, Benallaoua M, et al. Activation of the peroxisome proliferator-activated receptor alpha pathway potentiates interleukin-1 receptor antagonist production in cytokine-treated chondrocytes. *Arthritis Rheum*. 2006;54:1233–45.

13. Sasaki H, Takayama K, Matsushita T, Ishida K, Kubo S, Matsumoto T, et al. Autophagy modulates osteoarthritis-related gene expression in human chondrocytes. *Arthritis Rheum.* 2012;64:1920–8.
14. Caramés B, Taniguchi N, Otsuki S, Blanco FJ, Lotz M. Autophagy is a protective mechanism in normal cartilage, and its aging-related loss is linked with cell death and osteoarthritis. *Arthritis Rheum.* 2010;62:791–801.
15. Chen X, Gong W, Shao X, Shi T, Zhang L, Dong J, et al. METTL3-mediated m(6)A modification of ATG7 regulates autophagy-GATA4 axis to promote cellular senescence and osteoarthritis progression. *Ann Rheum Dis.* 2022;81:87–99.
16. Chen Y, Lin J, Chen J, Huang C, Zhang Z, Wang J, et al. Mfn2 is involved in intervertebral disc degeneration through autophagy modulation. *Osteoarthr Cartil.* 2020;28:363–74.
17. Alvarez-Garcia O, Matsuzaki T, Olmer M, Plate L, Kelly JW, Lotz MK. Regulated in development and DNA damage response 1 deficiency impairs autophagy and mitochondrial biogenesis in articular cartilage and increases the severity of experimental osteoarthritis. *Arthritis Rheumatol.* 2017;69:1418–28.
18. Kamekura S, Hoshi K, Shimoaka T, Chung U, Chikuda H, Yamada T, et al. Osteoarthritis development in novel experimental mouse models induced by knee joint instability. *Osteoarthr Cartil.* 2005;13:632–41.
19. Zhou Y, Chen X, Qu N, Zhang B, Xia C. Chondroprotection of PPAR α activation by WY14643 via autophagy involving Akt and ERK in LPS-treated mouse chondrocytes and osteoarthritis model. *J Cell Mol Med.* 2019;23:2782–93.
20. Glasson SS, Chambers MG, Van Den Berg WB, Little CB. The OARSI histopathology initiative - recommendations for histological assessments of osteoarthritis in the mouse. *Osteoarthr Cartil.* 2010;18(Suppl 3):S17–23.
21. Cui X, Wang S, Cai H, Lin Y, Zheng X, Zhang B, et al. Overexpression of microRNA-634 suppresses survival and matrix synthesis of human osteoarthritis chondrocytes by targeting PIK3R1. *Sci Rep.* 2016;6:23117.
22. Elsaid KA, Zhang L, Shaman Z, Patel C, Schmidt TA, Jay GD. The impact of early intra-articular administration of interleukin-1 receptor antagonist on lubricin metabolism and cartilage degeneration in an anterior cruciate ligament transection model. *Osteoarthr Cartil.* 2015;23:114–21.
23. Dai L, Chen X, Lu X, Wang F, Zhan Y, Song G, et al. Phosphoinositide-specific phospholipase C γ 1 inhibition induces autophagy in human colon cancer and hepatocellular carcinoma cells. *Sci Rep.* 2017;7:13912.
24. Sanduja S, Feng Y, Mathis RA, Sokol ES, Reinhardt F, Halaban R, et al. AMPK promotes tolerance to Ras pathway inhibition by activating autophagy. *Oncogene.* 2016;35:5295–303.
25. Zheng CH, Levenston ME. Fact versus artifact: avoiding erroneous estimates of sulfated glycosaminoglycan content using the dimethylmethylene blue colorimetric assay for tissue-engineered constructs. *Eur Cell Mater.* 2015;29:224–36.
26. Poleni PE, Etienne S, Velot E, Netter P, Bianchi A. Activation of PPARs α , β/δ , and γ impairs TGF- β 1-induced collagens' production and modulates the TIMP-1/MMPs balance in three-dimensional cultured chondrocytes. *PPAR Res.* 2010;2010: 635912.
27. Wang J, Wang G, Sun GW. Role of PPAR α in down-regulating AGE-induced TGF- β and MMP-9 expressions in chondrocytes. *Genet Mol Res.* 2016. <https://doi.org/10.4238/gmr.15027963>.
28. Korbecki J, Bobiński R, Dutka M. Self-regulation of the inflammatory response by peroxisome proliferator-activated receptors. *Inflamm Res.* 2019;68:443–58.
29. Caramés B, Hasegawa A, Taniguchi N, Miyaki S, Blanco FJ, Lotz M. Autophagy activation by rapamycin reduces severity of experimental osteoarthritis. *Ann Rheum Dis.* 2012;71:575–81.
30. Wang Y, Zhang T, Xu Y, Chen R, Qu N, Zhang B, et al. Suppressing phosphoinositide-specific phospholipases C γ 1 promotes mineralization of osteoarthritic subchondral bone osteoblasts via increasing autophagy, thereby ameliorating articular cartilage degeneration. *Bone.* 2022;154: 116262.
31. Jin S, White E. Role of autophagy in cancer: management of metabolic stress. *Autophagy.* 2007;3:28–31.
32. Gardner OS, Dewar BJ, Earp HS, Samet JM, Graves LM. Dependence of peroxisome proliferator-activated receptor ligand-induced mitogen-activated protein kinase signaling on epidermal growth factor receptor transactivation. *J Biol Chem.* 2003;278:46261–9.
33. Gardner OS, Dewar BJ, Graves LM. Activation of mitogen-activated protein kinases by peroxisome proliferator-activated receptor ligands: an example of nongenomic signaling. *Mol Pharmacol.* 2005;68:933–41.
34. Wang J, Wu GS. Role of autophagy in cisplatin resistance in ovarian cancer cells. *J Biol Chem.* 2014;289:17163–73.
35. Li T, Xu XH, Tang ZH, Wang YF, Leung CH, Ma DL, et al. Platycodin D induces apoptosis and triggers ERK- and JNK-mediated autophagy in human hepatocellular carcinoma BEL-7402 cells. *Acta Pharmacol Sin.* 2015;36:1503–13.
36. Ravingerová T, Carnická S, Nemčėková M, Ledvényiová V, Adameva A, Kelly T, et al. PPAR- α activation as a preconditioning-like intervention in rats in vivo confers myocardial protection against acute ischaemia-reperfusion injury: involvement of PI3K-Akt. *Can J Physiol Pharmacol.* 2012;90:1135–44.
37. Lu Q, Yan S, Sun H, Wang W, Li Y, Yang X, et al. Akt inhibition attenuates rasfonin-induced autophagy and apoptosis through the glycolytic pathway in renal cancer cells. *Cell Death Dis.* 2015;6: e2005.
38. Dou Z, Chattopadhyay M, Pan JA, Guerriero JL, Jiang YP, Ballou LM, et al. The class IA phosphatidylinositol 3-kinase p110- β subunit is a positive regulator of autophagy. *J Cell Biol.* 2010;191:827–43.

Publisher's Note

Springer Nature remains neutral with regard to jurisdictional claims in published maps and institutional affiliations.

Ready to submit your research? Choose BMC and benefit from:

- fast, convenient online submission
- thorough peer review by experienced researchers in your field
- rapid publication on acceptance
- support for research data, including large and complex data types
- gold Open Access which fosters wider collaboration and increased citations
- maximum visibility for your research: over 100M website views per year

At BMC, research is always in progress.

Learn more biomedcentral.com/submissions

